

Pedestrian-level wind conditions around buildings for wind comfort assessment

J. Steer, S. W. Li, N. Morcom, S. Jucius, F. Ghanadi and M. Arjomandi

School of Mechanical Engineering
University of Adelaide, Adelaide, South Australia 5005, Australia

Abstract

The practice of investigating the pedestrian level wind environment, so called wind engineering, is now ubiquitous. Many city case studies exist in literature but few systematic studies of common urban architectural features exist. Among these common features is the simple channel which is common in large cities and has been well documented in literature as leading to significant wind speed increases. This study investigates the effects of adding a blockage at the channel inlet on observed velocities in the channel centerline on 1:100 scale with a view to applying the results to full scale. Time averaged velocity profiles were used to investigate the effect of blockage size and channel width on wind speed amplification. It was found that counter-intuitively, the size of the blockage at the inlet is not proportional to the size of the peak velocity reduction in the channel. The largest blockage created a minimum flow speed reduction ($K = 0.98$) for a channel width of 200mm. It was outperformed by the smallest blockage for a channel width of 300mm where a greater speed reduction was observed ($K = 1.04$). It was found that for buildings nearing the interaction flow regime the addition of a blockage has negligible effect on speed.

Introduction

When a city's population increases, passages for thoroughfare between buildings become more common. A consensus in the field of wind engineering is that pedestrian level wind speeds in such passages can be elevated significantly beyond what would be considered comfortable by established global criterion. As the city is constructed with multiple different sized passages that are surrounded by buildings [1], a practical approach to investigate the effect of a passage is by first modelling two idealised buildings with a given sized gap. The so called channelling effect was studied by Blocken et al. [2] where it was characterised for the general case in terms of building influence scale (S) and amplification factor (K_{max}). Hence, the aim of this study will first be to validate these channelling results.

These studies, although comprehensive, have not attempted to provide methods to negate the channelling effect which in certain configurations increases the pedestrian level wind speed by over 40% [2]. Whilst significant research attention has been devoted to the analysis of this phenomenon, little has been dedicated to the development of a feasible solution. The effects of blockage ratio on flow speed at pedestrian level have yet to be analysed in general. Thus, the scope of this paper is to investigate the benefits to pedestrian comfort of the addition of a blockage at the inlet to passages between buildings. A relationship between the passage blockage ratio (B) and the maximum amplification factor along the passage centerline (k_{max}) will be determined for a variety of passage widths based on wind tunnel data and numerical modelling. These general findings can inform the future study of specific cases or streets.

Pedestrian wind comfort studies have been conducted throughout developed cities around the world, from a small scale modelling of single buildings to large scale central business district analysis [3]. High wind speeds at ground level have been shown

to influence the shopping choices of pedestrians [4]. Kadic et al. have reported that when wind speeds are below 2 km/h people are likely to spend more time in retail stores, restaurants and shopping malls, leading to a 21% increase in sales [5]. Teerayut et al. suggest that such an increase in sales is likely to correlate with the performance of the local economy and therefore it is in the interest of municipal governments to implement methods to reduce wind speeds.

In Sydney, Australia, there are a multiplicity of wind engineering consultants who utilise computational fluid dynamics modelling and experimental techniques to research the impact of proposed building projects on pedestrian level wind speeds [6]. A case study of the Carlton Connect development in Melbourne, Australia [7], found that the strategic inclusion of tall porous screens, living walls and densely foliated trees in the building campus could lead to a reduction in observed wind speeds. Similar observations have been made by Willemsen et al. [8], who classify buildings as requiring professional wind comfort assessment when the local surface area is not "covered for 20% or more with obstacles like trees (tops) and buildings up to a radius of 300 meters." It is common knowledge that trees can provide relief from high wind speeds [9]. Researchers in Niigata, Japan, have shown via extensive numerical analysis that planting trees near pedestrian walkways can reduce wind speeds to below 70% of what would otherwise be observed [10, 11].

In Toronto, Canada, several universities have pooled their resources and constructed a 3D model of the financial district to investigate the wind speed change caused by building development over the past 70 years [12]. Researchers backtracked the development of the city and built a computational model of the city from 1940 to 2015 with 10-20 year increments. In this case researchers were able to achieve agreement between experimental data [13, 14] and their numerical model to the extent that qualitative conclusions about flow behaviour could be drawn. However, the complexity of the geometry prevented complete agreement. It was concluded that high rise buildings can increase average wind speeds in main streets and small passage ways and suggestions were provided to minimise the wind speed amplification by constructing new buildings in strategic locations.

In each of these studies individual cases of new buildings were analysed but no concrete conclusions about the general case could be offered. Fundamental techniques for mitigating wind speed increases in urban environments remain as yet unknown and require in depth analysis via a series of small scale wind tunnel experiments.

Experimental Setup

Methodology

Experimental measurements were gathered in the wind engineering test section of the Thebarton Wind Tunnel, which has a $3 \times 3m^2$ cross-sectional area and can produce a boundary thickness of 1.2m. Figure 1 shows the schematic layout of the passage setup fixed on a stand with an elliptical leading edge for

minimal flow separation and boundary layer development [16]. The base was placed at a distance of 13 m from the flow straighteners at beginning of the test section. The base was constructed from plywood with width of 1.6 m, length of 0.72 m and raised 0.25 m above the wind tunnel surface. The boxes used to construct the channel had a dimension of 0.37 m (L) and were not permanently fixed to the base to allow the width and length of the channel to be adjusted. Blockages of dimension 5 x 15 cm, 10 x 15 cm and 20 x 15 cm were placed at a distance of 4.5 cm in the stream wise direction from the inlet to the channel. These blockages will be referred to as blockages 1, 2 and 3 in order of increasing size. The free stream turbulence intensity at the inlet to the passage on the center was approximately 3%.

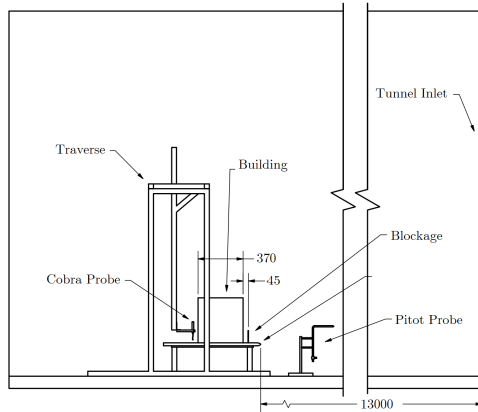


Figure 1: Diagram showing the relative arrangement of pressure taps along the centerline of the passage

The free-stream Reynold's number Re_∞ based on box width and free-stream velocity U_∞ was varied in a range between 125,000 and 220,000. Passage width was varied between 0.25 and L .

Flow Measurement Technique

A Turbulent Flow Instrumentation (TFI) Cobra pressure probe was used to measure the flow in the centerline of the passage. The multi-hole probe with 2.5 kPa pressure transducers was calibrated by the manufacturer to allow flow measurements up to 90 m/s and operate at a sampling frequency of up to 2 kHz. The probe was able to resolve the three orthogonal components of velocity and static pressure, as long as the flow vector was contained within a cone of 45 around the probe axis. Vertical velocity profile measurements were obtained using a high-frequency Cobra probe attached to a traverse system. A linear actuator attached to an Arduino Uno micro-controller was used to collect time averaged data over 20 second periods at 10 locations at 5 cm intervals at a sample rate of 1500 Hz.

A pitot probe was placed upstream of the test setup to record the free stream velocity. 16 taps of inner diameter 1.5 mm were situated along the centerline of the passage. The first tap was located 75 mm ahead of the passage entrance with the remaining taps approximately uniformly distributed at 30 mm spacing. The taps were connected to a Scanivalve DSA-3217 pressure transducer with a sampling frequency of 1000 Hz. Time-averaged results were obtained over a period of 20 seconds. The Scanivalve reference channel was connected to the total pressure channel on a pitot probe in order to record dynamic pressure. Figure 2 shows the relative locations of pressure taps on the surface of the model.

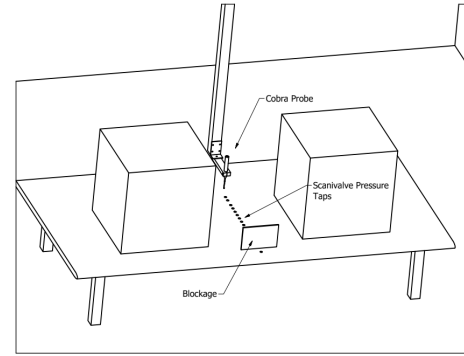


Figure 2: Schematic diagram of the passage setup with blockage, cobra probe, traverse and pressure taps.

Amplification Factor & Influence Scale

The degree to which the flow is accelerated by a given architectural feature is defined in literature as the amplification factor K [2]. Amplification factor is the ratio between the point velocities obtained for a given test geometry with and without architecture. The amplification factor is therefore calculated as:

$$K = \frac{U}{U_0} \quad (1)$$

The building influence scale was defined by Wilson [15] for estimating dimensions of flow recirculation regions on building roofs. By analysis of a range of wind tunnel measurements, Stathopoulos et al. (1992) found that $K_{pcl,max}$ seems to be an almost universal function of the ratio w/S , where w is the passage width and S is the building influence scale, defined as:

$$S = (B_L B_S^2)^{\frac{1}{3}} \quad (2)$$

B_L and B_S are the longest and shortest dimensions of the building respectively. K and S are used to non-dimensionalize experimental results.

Results & Discussion

Non-Dimensionalized Clean Channel Results

Figure 3 shows the maximum amplification factors (K_{max}) plotted against the width to building influence factor ratio (w/S) for the cases where there is no blockage. Equation 3 has been fitted to the data:

$$K_{max} = 1.205 \left(\frac{w}{S} \right)^{-0.09} \quad (3)$$

The maximum observed amplification factor decreases with larger values of w/S which is consistent with experimental results from Blocken et al. Relations such as 3 can be used by town planners to predict the wind speed increase for a new building based on it's geometry and incident wind speed. The spread of data about the trendline is likely due to the oscillating nature of the flow as the presence of Von-Karman vortex street has been observed for this configuration in literature [2].

Time Averaged Centreline Amplification Factors

Figure 4 shows the observed K values in the stream wise direction for the clean passage and three blockage cases for a Reynold's number of 170,000 and a passage width of 100 mm.

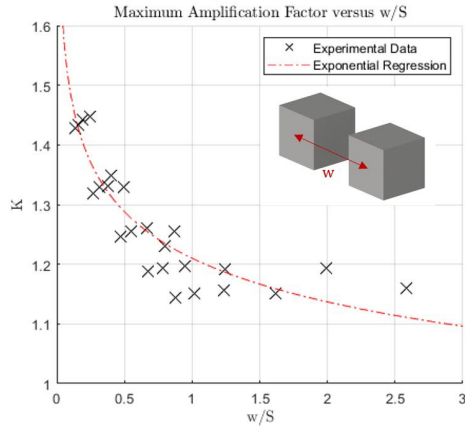


Figure 3: Maximum amplification factor versus non-dimensionalized building geometry

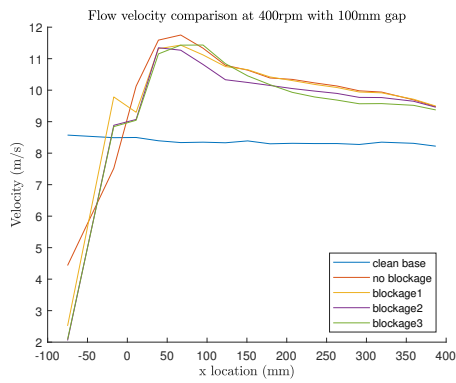


Figure 4: Time-averaged velocities at a passage width of 100 mm

Ahead of the passage inlet the addition of a blockage leads to an increase in amplification factor due to vortex production and recirculation. Figure 5 shows the obtained surface velocity profiles observed for the case where the gap width is 200 mm. In each of the blockage profiles an increase in velocity is observed immediately behind the blockage, followed by a decrease downstream.

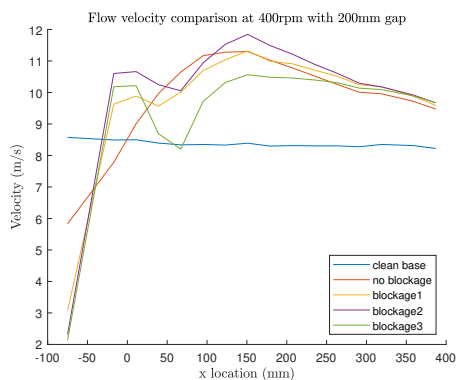


Figure 5: Time-averaged velocities at a passage width of 200 mm

Many similarities exist between the 200mm channel width case and the larger channel width cases. Figures 6 and 7 show the velocity profiles observed for 300 mm and 400 mm gap widths

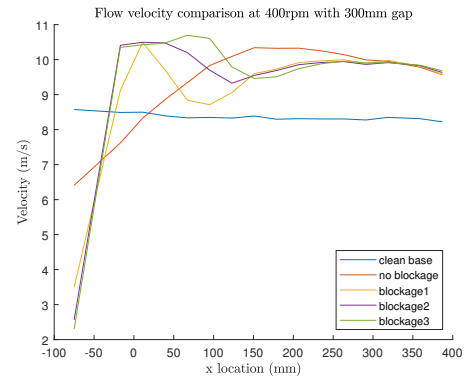


Figure 6: Time-averaged velocities at a passage width of 300 mm

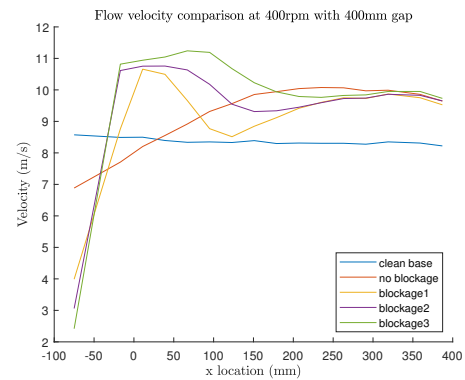


Figure 7: Time-averaged velocities at a passage width of 400 mm

respectively. A peak is always observed within the passage and at some x position the blockages begin to provide some positive benefit by reducing the amplification factor when compared to the clean case. The positions at which this transition occurs are summarised in Table 1 .

	Transition Location			
	100 mm	200 mm	300 mm	400 mm
Blockage 1	11	39	67	95
Blockage 2	11	67	95	123
Blockage 3	11	39	123	179

Table 1: Position of the transition between blockage feature providing larger amplification factors to smaller when compared to the clean case

Table 1 shows that a larger blockage size leads to a delayed transition. This suggests that the transition location is dictated by the size of the vortex generated by the blockage and that transition occurs when the flow from the vortex reattaches to the model surface. This theory is supported by the fact that in all cases the amplification factors approach that of the clean case after transition occurs, indicating reattachment. Figure 8 shows an illustration of the pattern of streamlines that is believed to exist behind the blockage for the cases of greater than 200 mm width.

The placement of a blockage at the passage inlet has a significant impact on the centerline velocity profile via the creation of a vortex in the wake. The extent of the vortex is proportional to blockage size and channel width. The reattachment length of

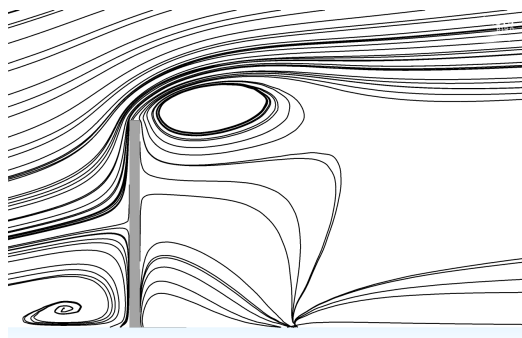


Figure 8: Illustrated flow behaviour

the vortex is also dependent on free stream velocity. However, due to the limited collected data, the diameter and the vortex oscillation frequency is yet to be found. When the flow is transitional between the resistance to the interaction regime [2] as in Figure 4 the addition of a blockage does not reduce the amplification factors in the centerline of the passage significantly from the clean case.

The magnitudes of the maximum and minimum amplification factor are clearly dependent on blockage size, however a larger blockage size does not always correspond to a larger reduction as was expected. The larger blockage produces a greater reduction in the smaller channel (Figure 5) in the interaction regime [2] where a minimum amplification factor of 0.98 is observed compared with 1.14 and 1.20 for blockages 1 and 2 respectively. However, in the larger channels the smallest blockage is dominant (Figures 6, 7). For a channel width of 300 mm a minimum amplification factor of 1.04 is observed for blockage 1, compared with 1.12 for both 2 and 3. This indicates that there may exist an "ideal" blockage size that provides the maximum reduction for each channel configuration.

Counter intuitively, the size of the blockage is not proportional to the size of the peak velocity reduction in the channel. Whilst the largest blockage generated a minimum amplification factor of 0.98 for a channel width of 100 mm, it was outperformed by the smallest blockage for larger values of w . This finding lends credibility to the notion that small, non-invasive street blockages can realise tangible reductions in pedestrian level wind speeds. This also suggests that for a given channel geometry there exists a corresponding blockage size that provides maximum velocity reduction that is not necessarily the largest possible blockage.

Conclusion

Wind tunnel results have shown that the placement of a rectangular blockage at the inlet to a channel generates a vortex within the channel. The size of the vortex is proportional to the frontal area of the blockage and width of the channel. The magnitude of the velocity change along the surface centerline of the passage is dictated by the size of the vortex produced. Experimental data suggests that a street blockage may be ineffective for reducing wind speeds in narrow streets.

Further full-scale investigation accompanied by numerical modelling is required to put these concepts into practice. The oscillation frequency of the produced vortex is yet to be investigated and the collection of transient data may yield further insight into the mechanisms governing the flow behaviour observed in this experiment and ways to reduce wind speeds at pedestrian level.

Acknowledgements

The members of the wind comfort study of Adelaide would like to thank Marc Simpson and Azadeh Jafari for their assistance at the Thebarton Wind Tunnel facility. Furthermore, acknowledgement is given to the technical workshop staff, especially Gary Bowman and Robert Dempster for constructing required components for testing. Additionally, CFD assistance from Nima Sedaghatizadeh was greatly appreciated.

References

- [1] Stoesser, T., Mathey, F., Frohlich, J. and Rodi, W., Lesof flow over multiple cubes, *Ercoftac Bulletin*, **56**, 2003, 15-19.
- [2] Blocken, B., Carmeliet, J. and Stathopoulos, T., Cfd evaluation of wind speed conditions in passages between parallel buildings effect of wall-function roughness modifications for the atmospheric boundary layer flow, *Journal of Wind Engineering and Industrial Aerodynamics*, **95**, 2007, 941-962.
- [3] Kang, G., Kim, J.-J., Kim, D.-J., Choi, W. and Park, S.-J., *Development of a computational fluid dynamics model with tree drag parameterizations: Application to pedestrian wind comfort in an urban area*, *Building and Environment*, **124**, 2017, 209-218.
- [4] Horanont, T., Phithakkitnukoon, S., Leong, T. W., Sekimoto, Y. and Shibasaki, R., *Weather effects on the patterns of peoples everyday activities: a study using gps traces of mobile phone users*, *PLoS one*, **8**, 2013, e81153.
- [5] Kadic-Magljalic, S., Micevski, M., Lee, N., Boso, N. and Vida, I., *Three levels of ethical influences on selling behavior and performance: Synergies and tensions*, *Journal of Business Ethics*, 1-21.
- [6] Paetzold, J., *Wind tunnel test for: Martin place over station*, *Wind Engineering and Air Quality Consultants*, 1015.
- [7] Ltd, W. C. P., *Pedestrian wind environment study carlton connect initiative, WD086-02F02(REV6)- WE REPORT*.
- [8] Willemsen, E. and Wisse, J. A., *Design for wind comforting the Netherlands: Procedures, criteria and open research issues*, *Journal of Wind Engineering and Industrial Aerodynamics*, **95**, 2007, 1541-1550.
- [9] Beckett, K. P., Freer-Smith, P. and Taylor, G., *Particulate pollution capture by urban trees: effect of species and wind speed*, *Global change biology*, **6**, 2000, 995-1003.
- [10] Mochida, A. and Lun, I. Y., *Prediction of wind environment and thermal comfort at pedestrian level in urban area*, *Journal of wind engineering and industrial aerodynamics*, **96**, 2008, 14981527.
- [11] S.Yoshida, Ooka, R., Mochida, A., S. and Tominaga, Y., *Development of three dimensional plant canopy model for numerical simulation of outdoor thermal environment*.
- [12] Adamek, K., Vasan, N., Elshaer, A., English, E. and Bitsuamlak, G., *Pedestrian level wind assessment through city development: A study of the financial district in Toronto*, *Sustainable Cities and Society*, **35**, 2017, 178-190.
- [13] Dagnew, A. and Bitsuamlak, G. T., *Computational evaluation of wind loads on buildings: a review*, *Wind Struct*, **16**, 2013, 629-660.

- [14] Weerasuriya, A., Computational fluid dynamic (Cfd) simulation of flow around tall buildings, Engineer: Journal of the Institution of Engineers, Sri Lanka, **46**.
- [15] Wilxon, D., *Airflow around buildings, A SHRAE Handbook of Fundamentals*, **14**, 1989, 1-18.
- [16] Narasimha, R. and Prasad, S., *Leading edge shape for flatplate boundary layer studies, Experiments in Fluids*, **17**, 1994, 358360.